Generation and characterization of multi-phase AC arc for in-flight melting of granulated glass raw materials

Takayuki Watanabe[1], Yaochun Yao[2], Kazuyuki Yatsuda[1], Tsugio Matsuura[3]

[1]*Department of Environmental Chemistry and Engineering, Tokyo Institute of Technology, Japan*
[2]*National Engineering Lab of Vacuum Metallurgy, Kunming University of Science and Technology, China*
[3]*Industrial Technology Center of Fukui Prefecture, 61 Kawai-Washizuka, Japan*

Abstract: A stable 12-phase AC arc was generated and developed to apply to glass in-flight melting for the purpose of energy saving and emission reduction. The arc behavior was characterized by image analysis. Results show that plasma shape can be controlled by the electrode configuration. The luminance area with high-temperature region and its fluctuation reflect the change of arc discharge behavior.

Keywords: Multi-phase AC arc, Thermal plasma, In-flight melting, Image analysis

1. Introduction

The glass industry is a large global industry that annually produces more than 100 million tons of glass products such as sheet glass, container glass, fiber glass, optical glass, and so on [1]. The typical melting system for glass is refractory-lined melting furnace, fired by air and natural gas or oil as fuel, which has been used over 140 years in glass industry [2]. In the air-fuel fired furnace, the heat transfer from the burner flame to glass melt is so low that the conventional melting technology is energy intensive and time consuming, especially, in the melting and refining process. In addition, lots of emissions are produced during melting due to the usage of fossil fuel, which brings more environmental problem.

The use of thermal plasmas in material processing is becoming an increasingly active and attractive field. The potential applications of thermal plasma processing in industries cover a wide range of activities, such as spray coating. extraction of metals, remelting and refining of metals or alloys, synthesis of advanced materials, as well as treatment of toxic and hazardous waste [3-6]. Compared with other thermal plasmas, multi-phase alternating current (AC) arc possesses the following advantages: high energy efficiency, large plasma volume, low velocity, easy scale up, and low cost [7-9]. The high temperatures of the plasma make it possible to melt glass raw materials quickly to decrease the melting time. Lessening the formation of bubbles in molten glass is an effective way to shorten the fining time. It can be achieved by releasing the decomposed gas from raw material during the powder flying. Under the New Energy and Industrial Technology Development Organization (NEDO) project, an innovative in-flight melting technology with multi-phase AC arc was successfully developed for glass industry [10-12].

In this study, a stable 12-phase AC arc was generated by transformers at a commercial electric power system and the arc behavior was characterized by using a high speed video camera. The effect of flow rate of shield gas and electrode configuration on the arc behavior and in-flight melting behavior of granulated raw material was investigated.

2. Experimental

A new type of arc plasma reactor with 12-phase AC discharge has been developed to get stable and continuous arc by the transformers for converting from 3-phase AC to 12-phase AC, as shown in Fig. 1. The input of the three-phase power supply is connected to 200 V (50 Hz) commercial power lines. The primary coils of transformers are divided into two parts: one is the Δ connection and the other is the Y connection. The turn's ratio of the windings between the primary and secondary coils of the Δ connection transformer was designed $1/\sqrt{3}$. The 12-phase power supply can be realized by the combination of these circuits, then, each line is connected directly to the corresponding electrodes [9].

The schematic diagram of experimental setup is shown in Fig. 2. It consisted of 12 electrodes, reaction chamber, powder feeder, and AC power supply. The 12 electrodes was symmetrically arranged by the angle of 30 deg and divided into two layers, upper 6 electrodes and lower 6 electrodes. The electrode in diameter of 3.2 mm was tungsten (98%) with thoria (2%). City water was used to cool the electrode bodies, and argon (99.99%) was

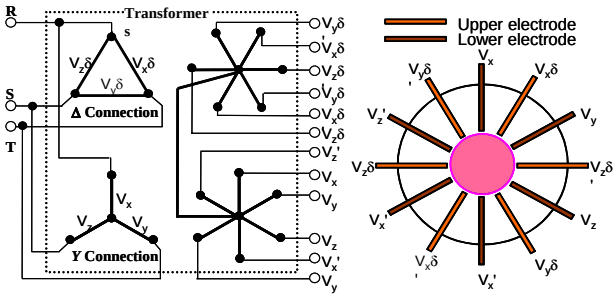

Fig.1 Electrical circuit diagram and connection diagram of 12-phase AC arc reactor

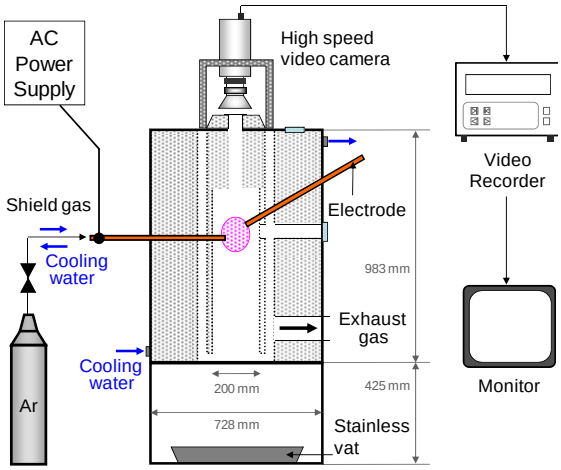

Fig.2 Schematic diagram of the experimental setup

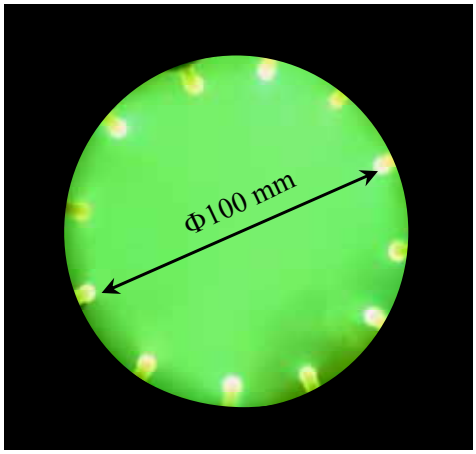

Fig.3 12-phase AC arc discharging

injected around the electrodes to prevent them from oxidation. Fig. 3 displays the generated 12-phase AC arc. The input power was 50 kW, voltage 195 V and current 300 A. The discharge voltage and current of each electrode were 30-45 V and 80-130 A, respectively. The diameter of arc was about 100 mm; the distance between two layers of the electrodes was 50 mm.

The mixture of Na_2CO_3, $CaCO_3$, and SiO_2 was prepared into granulated powder for soda-lime glass by spray dry method. The initial powder with 100 μm in average diameter was injected into the plasma at the feed rate of 30 g/min with air carrier gas of 20 L/min by a powder feeder. The powders treated by the 12-phase arc were quenched on the stainless steel pan at a distance of 1050 mm below the nozzle.

The structures of the powders were determined by X-ray diffractometry (XRD) on Miniflex (Rigaku) with Cu K_α radiation at 30 kV and 15 mA. The data were collected for 3-90° range as 2θ with a step size of 0.02^o and a scan speed of 4° min^{-1}. The particle size distribution of the powders was obtained by measuring 200 particles with IX71 microscope (Olympus).

The discharge behavior of the 12-phase arc with two kinds of electrode configurations was characterized by a high speed video camera (HSV-500C^3, NAC) installed on the top of the reaction chamber. It consists of a color digital camera, a video recorder, and a monitor. The arc discharge behavior was recorded at a speed of 500 fps (frames per second) and a shutter speed of 0.1 μs. A continuous images were recorded to observe the arc discharge behavior, and then the captured video images were decomposed to individual image at an interval of 2 ms, each of which was subjected to the following image analysis (as shown in Fig. 4).

a. Import the image
b. Set the image size (the discharge region)
c. Convert the image into grayscale mode
d. Convert the grayscale image into binary image by setting luminance value at 50 to estimate the luminance area according to pixel scale

3. Results and discussion

Fig. 5 illustrates two kinds of electrode configurations and their discharge behavior in a cycle. The number marked on figure indicates the phase shifting order. All the electrodes are arranged counterclockwise according to the phase sequence in configuration *I* (normal discharge). For configuration *II*, the upper 6 electrodes keep fixed and the 6 lower electrodes rotate 180° in clockwise. Fig. 5 (a) and (f) have the same discharge behavior for every electrode configuration, indicating a complete discharge cycle every 20 ms. For both configurations, the maximum phase difference exists in the opposite electrodes. The discharge mainly takes place

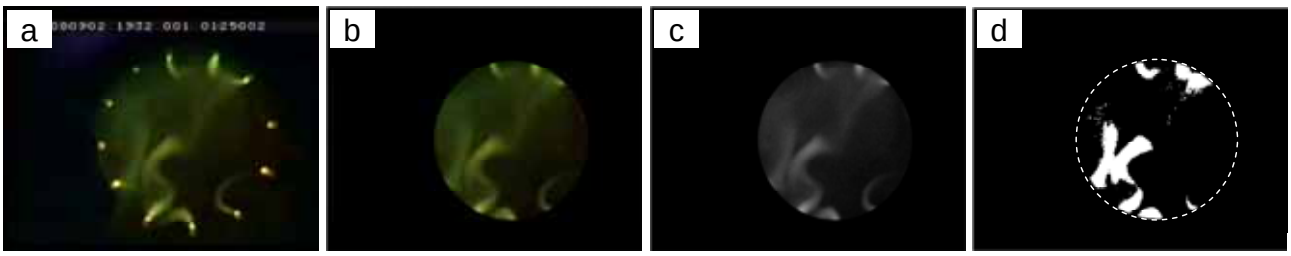

Fig.4 Procedure for image analysis of luminance area generated by 12-phase AC arc

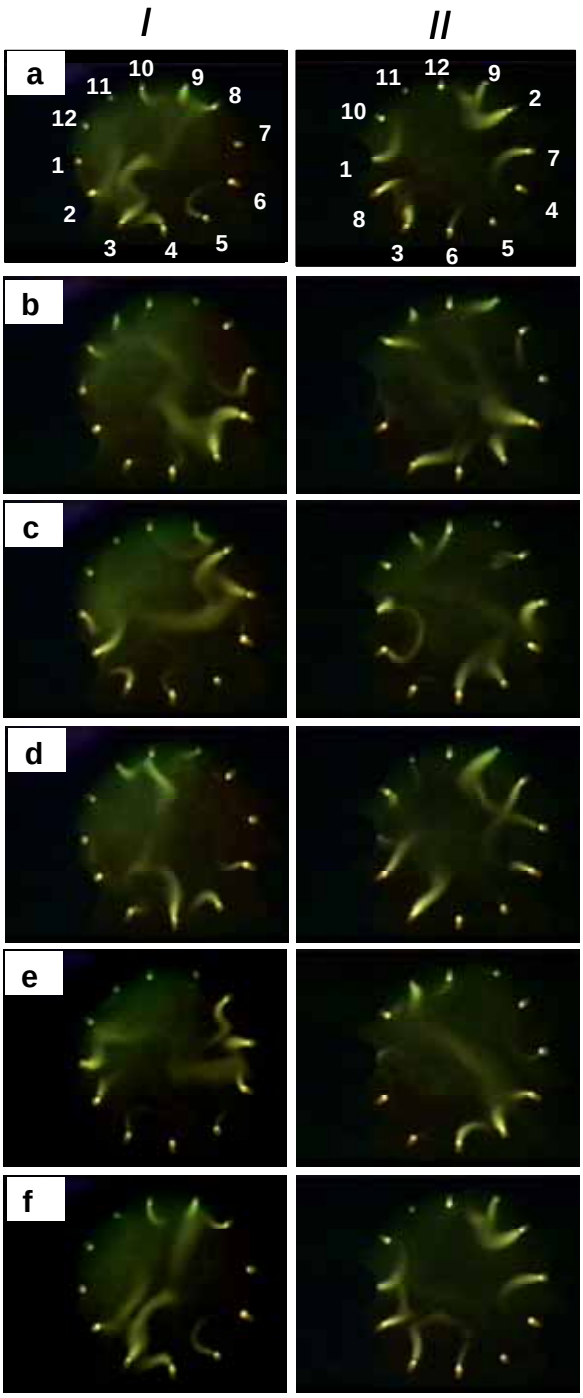

Fig.5 12-phase arc discharge with different electrode configuration in a cycle (60 l/min argon sheath gas): (a) 0 ms, (b) 4 ms, (c) 8 ms, (d) 12 ms, (e) 16 ms, (f) 20 ms

between two opposite electrodes and rotates in counterclockwise direction in the cases of configurations *I*. In contrast, the discharge almost occurs between close electrodes in configuration *II*. From Fig. 5, the luminance of arc in configuration *I* is larger than that in configuration *II*.

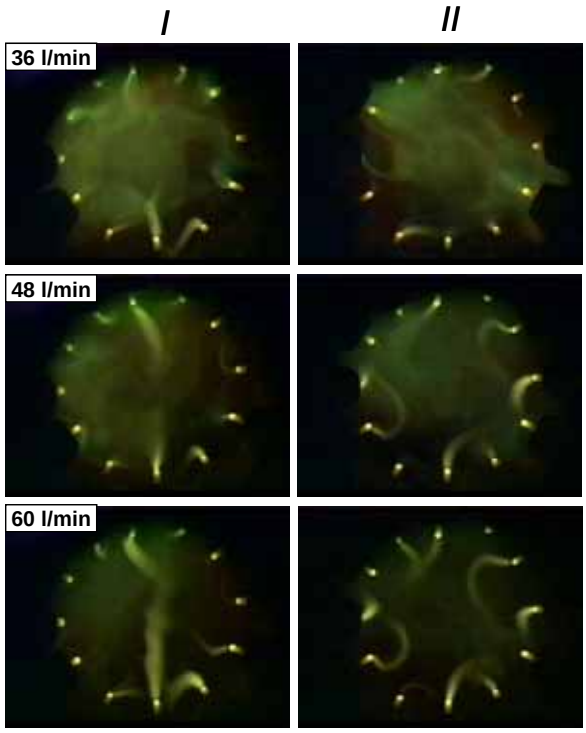

Fig.6 Arc discharge behavior at different flow rates of argon sheath gas

Fig. 6 shows the arc discharge behavior under different flow rates of sheath gas. As the flow rate of sheath gas increases, the luminance area becomes smaller and the plasma flame becomes narrower and longer. The flow rate of sheath gas prolongs the plasma flame and makes the plasma flame close to the arc center, indicating a higher plasma temperature formed on the arc center.

The ratio of luminance area is defined as the luminance area divided by the whole area, as described in Fig. 4 (d). Fig. 7 shows the fluctuation of the ratio of luminance area as a function of discharge time at different flow rates of sheath gas. The ratio decreases with an increase in flow rate of sheath gas. At small flow rate of sheath gas, broad flame of plasma leads to a slow fluctuation of the ratio of luminance area. Comparison between the area ratios of configuration *I* and *II* at the same flow rate, the ratio in configuration *I* is higher than that in configuration *II*. This reveals the temperature distribution in configuration *I* is more uniform. These evaluated results are in agreement with the discharge images.

The variation of vitrification and average particle size of samples treated at different flow rates of sheath gas is shown in Fig. 8. The vitrification degree was measured by the internal standard method with XRD [13]. At larger flow rate of sheath gas, the vitrification degree is higher and the particle size is smaller. It is noted that the shrinkage of particle is related with its vitrification degree; higher vitrification degree, more shrinkage of

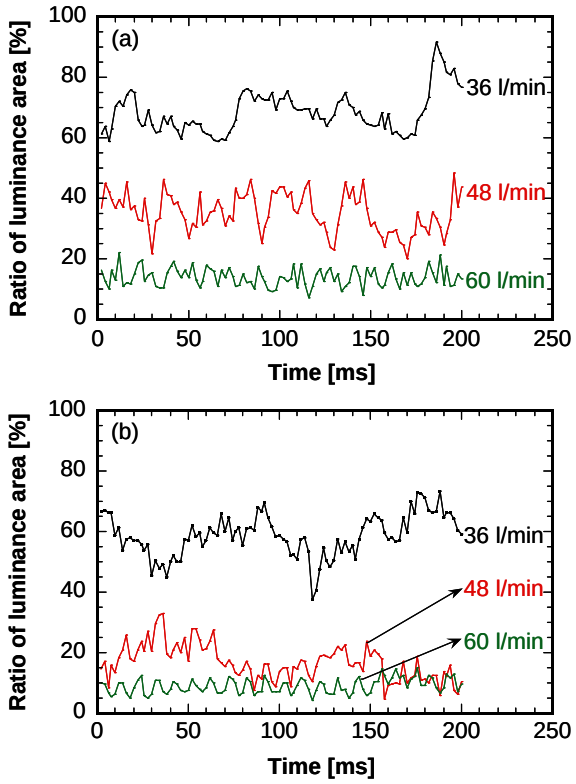

Fig.7 Fluctuation of luminance area ratio at different flow rates of sheath gas: (a) configuration *I*, (b) configuration *II*

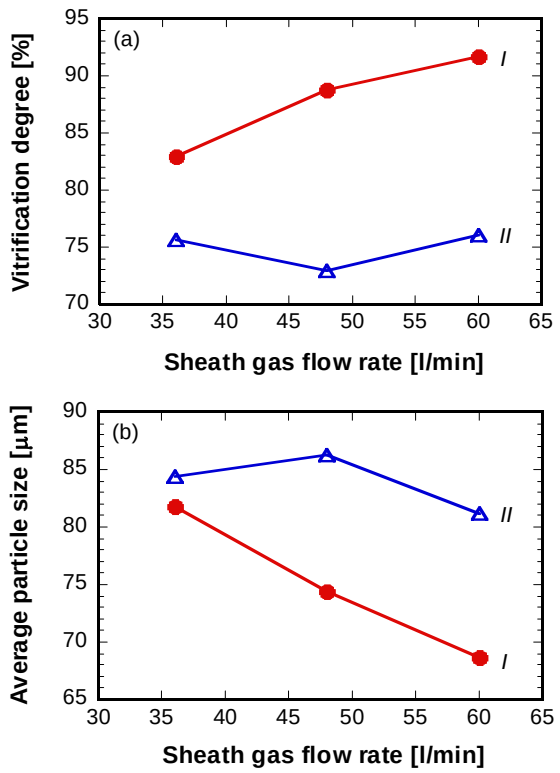

Fig.8 Variation of vitrification and average particle size of samples: (a) vitrification degree, (b) average particle size

particles. The shrinkage of particle size after heating is attributed to the reduction of material porosity. Although larger flow rate of sheath gas results in stronger cooling effect on arc edge, longer plasma flame makes the center temperature of arc improved. Hence, higher temperature on arc center causes higher vitrification degree in configuration *I*. The special discharge characteristic between near electrodes in configuration *II* brings about lower center temperature which explains its lower vitrification degree.

4. Conclusions

A stable 12-phase AC arc was generated and characterized using image analysis. Study shows that the electrode configuration and sheath gas have strong effects on the arc and melting behavior. Different electrode configurations results in various discharge behaviors. The vitrification of raw material most depends on the center temperature of plasma, so the vitrification degree of powders treated in configuration *I* is high. With the flow rate of sheath gas increasing, the average area ratio decreases and the vitrification degree increases.

Acknowledgements

The financial support provided by Energy Innovation Program of NEDO (New Energy and Industrial Technology Development Organization) is gratefully acknowledged.

References

[1] G. Tincher, Am. Ceram. Soc. Bull., **83,** 33 (2004).
[2] C. P. Ross, Am. Ceram. Soc. Bull., **83,** 18 (2004).
[3] J. Heberlein, Pure Appl. Chem., **74**, 327 (2002).
[4] P. Fauchais, G. Montavon, M. Vardelle, and J. Cedelle, Surf. Coat. Technol., **201**, 1908 (2006).
[5] A. Nezu, T. Morishima, amd T. Watanabe, Thin Solid Films, **435**, 335 (2003).
[6] M. Sakano, M. Tanaka, T. Watanabe, Thin Solid Films, **386,** 189 (2001).
[7] K. Matsumoto, Plasma Sources Sci. Technol., **5**, 245 (1996).
[8] R.J. Cogdell, Foundations of Electrical Engineering, Englewood Cliffs, NJ: Prentice-Hall (1990).
[9] T. Matsuura, K. Taniguchi, and T. Watanabe, Thin Solid Films, **515**, 4240 (2007).
[10] Y. Yao, M.M. Hossain, T. Watanabe, F. Funabiki, and T. Yano, Chem. Eng. J., **139,** 390 (2008).
[11] Y. Yao, K. Yatsuda, T. Watanabe, F. Funabiki, and T. Yano, Chem. Eng. J., **144,** 317 (2008).
[12] Y. Yao, et al., Sci. Tech. Adv. Mater., **9**, 025013 (2008).
[13] D. E. Willis, Chromatographia, **5**, 42 (1972).